N84-26558

BURROWS ET AL.

LIMITS ON SOFT X-RAY FLUX FROM DISTANT EMISSION REGIONS

D. N. BURROWS, D. MC CAMMON, W. T. SANDERS AND W. L. KRAUSHAAR

Department of Physics, University of Wisconsin-Madison

Received 1984 May 7;

ABSTRACT

We use the all-sky soft X-ray data of McCammon et al. and the new N_H survey (Stark et al. to place limits on the amount of the soft X-ray diffuse background that can originate beyond the neutral gas of th e galactic disk. The X-ray data for two regions of the sky near the galactic poles are shown to be uncorrelated with the 21 cm column densities. Most of the observed X-ray flux must therefore originate on the near side of the most distant neutral gas. The results from these regions are consistent with X-ray emission from a locally isotropic, unabsorbed source, but require large variations in the emission measure of the local region over large angular scales.

Subject headings: interstellar: matter--galaxies: Milky Way- radio sources: 21-cm radiation - X-rays: sources

I. INTRODUCTION

The soft X-ray diffuse background (SXRB, $0.13 \lesssim E < 0.284$ keV) has been mapped over most of the sky (McCammon et al. 1983). Stars and non-thermal diffuse processes seem unlikely to be significant contributors to the SXRB (Williamson et al. 1974; Vanderhill et al. 1975; Levine et al. 1977; Rosner et al. 1981). The large soft X-ray flux observed in the galactic plane, which is opaque at these energies, requires that the SXRB at low latitudes originate in a nearby region of hot gas ($T \sim 10^6$ K). OVI observations have provided evidence for interstellar gas at somewhat lower temperatures (Jenkins and Meloy 1974; Jenkins 1978a,b), and current theoretical models of the interstellar medium (ISM) can accommodate widespread gas near 10^6K in the galactic disk that is maintained at a high temperature by supernovae (McKee and Ostriker 1977; Cox and Anderson 1982).

The SXRB is much brighter at high galactic latitudes than at low latitudes and is anticorrelated with 21 cm column densities on a global scale, particularly in the northern galactic hemisphere. The existence of an anticorrelation between $\frac{1}{4}$ keV X-rays and N_H has been known since the first soft X-ray observations of Bowyer, Field, and Mack (1968), but mechanisms responsible for this anticorrelation remain unclear.

An early model postulated flux from an extragalactic or halo source of emission which would be partially absorbed by the neutral gas of the galactic disk. We shall refer to models in which the spatial structure of the SXRB is the result of absorption of X-rays originating in distant emission regions as absorption models.

Evidence apparently inconsistent with absorption models comes from experiments designed to measure absorption of soft X-rays by the gas of the Magellanic Clouds (McCammon et al. 1971; McCammon et al. 1976; Long, Agrawal, and Garmire 1976). These experiments found no evidence for absorption of soft X-rays either by the neutral gas in the Magellanic clouds or by the galactic gas along the line of sight. These results do not conclusively rule out the absorption model, however, for the following reasons.

1. Spatial structure in the emission from a postulated galactic halo could conceivably compensate for the predicted intensity variations due to absorption by galactic gas.

2. There is without question local soft X-ray emission as evidenced by the measured intensity in the galactic plane. We have no evidence that this local emission is spatially structureless at any angular scale and it is conceivable that this local source has intensity variations that obscure the expected spatial absorption features.

3. The predicted X-ray absorption by galactic gas is very sensitive to possible misinterpretation of the 21 cm data because of the uncertain contribution of stray radiation from antenna side lobes to the measured H I column densities, particularly at high galactic latitudes.

Current interest in hot halo or fountain models (Shapiro and Field 1976; Chevalier and Oegerle 1979; Bregman 1980a, b; Cox 1981) and the availability of extensive X-ray data (McCammon et al. 1983) and of 21 cm measurements that are essentially free of stray radiation (Stark et al. 1984) have prompted us to re-examine the evidence for or against absorption models. We assume a very simple model in which the SXRB consists

of two components, one nearby and unabsorbed, the other remote and subject to absorption by the total column density of neutral gas measured at 21 cm (N_H).

Under these assumptions all features in the N_H map should have predictable effects on the measured soft X-ray intensity. For the purposes of this paper, we have chosen two relatively small patches of sky at high galactic latitudes. Both areas have reliable X-ray data with good statistical accuracy, as well as significant features in the N_H data. X-ray absorption, if it is present, should be unambiguously evident in these data. While accidental cancellation of absorption features by emission features in one area is conceivable, such a fortuitous circumstance in two more areas is most unlikely.

II. DATA

The X-ray data used in this analysis are from the Wisconsin all-sky survey of the SXRB. Maps of the sky in seven energy bands and complete experimental details are given in McCammon et al. (1983). A brief description of the experiment follows.

The survey consists of data from ten sounding rocket flights. Each payload carried two or three (depending on the flight) wire-walled proportional counters pressurized to about 800 T with P-10 gas (10% methane, 90% argon). One counter on each flight carried a boron-coated Formvar window. The low energy band defined by the window transmission characteristics of this counter is called the B band (0.13-0.188 keV at 20% of the peak response). Typically, the other counter carried a polycarbonate window. The low energy band from this counter is called the C band (0.16-0.284 keV at 20% of the peak response). The B band data were taken using a circular field of view that can be approximated by a triangular response function with $7\overset{\circ}{.}1$ FWHM. The field of view for the C band data corresponds to $7\overset{\circ}{.}8$ FWHM for a triangular response. (These are larger than the field of view for our higher energy bands, due to reflection of low energy X-rays by the collimators.)

In planning the analysis to be described here, we chose to concentrate our efforts on two portions of the entire data set, one from a rocket flight (25.051) that scanned near the north galactic pole (NGP) and one from another flight (13.049) that scanned near the south galactic pole (SGP). At these high galactic latitudes the X-ray transmission of the neutral gas is relatively large and the analysis should be particularly sensitive to any distant emission component. Both regions are devoid of significant discrete

soft X-ray sources and the data are of good quality, free from contamination by electrons or non-cosmic X-rays. Both regions are also included in the Crawford Hill 21 cm survey, described below. With a view towards good spatial coverage, statistical accuracy, and likely spatial uniformity of local emission, we limited the initial analysis to regions within 20° of $(\ell,b) \simeq (215^{\circ}, 85^{\circ})$ for flight 25.051 (see Fig. 2) and to within 20° of $(\ell,b) \simeq (284^{\circ}, -79^{\circ})$ for flight 13.049 (see Fig. 5). The data taken during these scans were binned so that each data point includes counts from a portion of the scan path no longer than $3\overset{\circ}{.}3$.

The 21 cm data used in this analysis are from the recently completed survey by Stark et al. (1984), which was made with the Crawford Hill horn antenna. The 21 cm profiles were integrated from -100 km s^{-1} to $+100$ km s^{-1} for this analysis. The Crawford Hill horn antenna has over 99.9% of its response within 10° of the main beam, which has a $2\overset{\circ}{.}5$ HPBW response (Penzias, Wilson, and Encrenaz 1970). It is therefore insensitive to 21 cm emission at large angles from the center of the main beam, and the data should be essentially free of contamination by stray radiation. A detailed examination of the structure in the Crawford Hill data from the regions of the sky used in this analysis suggests that adjacent scans at constant declination occasionally differ by as much as $\sim 1 \times 10^{19}$ cm^{-2}. A comparison of measurements made within $0\overset{\circ}{.}25$ of each other in directions with $N_H < 5 \times 10^{20}$ cm^{-2} indicates that the observations were repeatable to about $6 \times 10^{18} cm^{-2}$. Uncertainties of 10^{19} cm^{-2} in column density translate into 0.18 and 0.08 uncertainties in absorption optical depths for B and C band, respectively.

III. ANALYSIS

We wish to place limits on the fraction of the X-ray intensity observed at high latitudes that is absorbed by the neutral gas along the line of sight. We consider a simple model of the form

$$I(\ell,b) = I_L + I_D \exp(-\sigma_{eff} N_H(\ell,b)), \qquad (1)$$

where $I(\ell,b)$ is the X-ray count rate in the direction (ℓ,b); I_L is the count rate from a local (unabsorbed) emission component, which we assume does not vary significantly over the portion of the sky included in the analysis; I_D is the unabsorbed count rate from a distant emission component, which is located beyond all of the neutral gas in the line of sight, and which we assume does not vary over this limited portion of the sky; σ_{eff} is the effective X-ray absorption cross section; and N_H is the 21 cm column density in this direction. The model parameters, I_L, I_D, and σ_{eff}, were varied to provide the best fit to the observed count rate, and the method of Lampton, Margon, and Bowyer (1976) was used to derive confidence limits for the model parameters.

The distant emission component was calculated in the following manner. The field of view for each data point was divided into 89 lines of sight. A spectral model of X-ray emission from a plasma in collisional equilibrium with temperature $T = 10^{6.0}$ K and unit emission measure was assumed (Raymond and Smith 1977, 1979). For each line of sight, the column density of neutral gas was interpolated from the Crawford Hill data. The incident model spectrum was multiplied by the ISM transmission, the calculated atmospheric transmission (which exceeded 0.8 in all cases) and the

collimator response for each line of sight. The results were then summed, folded through the proportional counter response function, and binned into our standard broad energy bands for comparison with the data. The predicted count rates for emission from the local component were calculated similarly. The emission measures and σ_{eff} were then varied to determine for each X-ray energy band the best fit of the model given by equation (1) to the data.

We estimate the nominal interstellar absorption cross sections to be $\sigma_B = 1.8 \times 10^{-20}$ cm^2 and $\sigma_C = 0.8 \times 10^{-20}$ cm^2 for the B and C bands, respectively. These use the Brown and Gould (1970) compilation and have been averaged over the B and C energy bands for a $T = 10^6$ K spectrum of Raymond and Smith (1977, 1979). If there were no clumping of the interstellar gas on angular scales smaller than the Crawford Hill beam and if equation (1) represents an appropriate model, we would expect σ_{eff} values to agree with σ_B and σ_C. Smaller scale clumping would reduce the effective cross sections, and that is why we allowed values of σ_{eff} to vary as free parameters. We emphasize that our analysis procedure explicitly takes into account variations in N_H on angular scales larger than the Crawford Hill beam.

We introduce a clumping parameter, α, defined as

$$\alpha \equiv \frac{\sigma_{eff}}{\sigma}, \qquad (2)$$

which characterizes clumping of the neutral gas on angular scales unresolved by the Crawford Hill beam in terms of its effect upon the X-ray transmission of that gas. In particular, α accounts for the difference between the actual X-ray transmission of the gas in the Crawford Hill beam in a given

direction and the X-ray transmission predicted for the average column density measured by the Crawford Hill beam in the same direction. This is a "two-dimensional" clumping parameter that depends only on small angular scale variations in N_H. It does not directly describe the three-dimensional structure of the absorbing gas, although it is related to that structure. The relationship between α and measures of the three-dimensional gas structure depends on the geometry of the clumping, i.e., whether the neutral gas exists in the form of spherical clouds, sheets, filaments, or other shapes.

Estimates of α can be derived from H I column density measurements made at higher angular resolution than the Crawford Hill beam. Such estimates are made by mapping the H I column density over a region the size of the Crawford Hill beam, calculating the average X-ray transmission of this region, and comparing it to the X-ray transmission of the average column density in the same region. The clumping parameters due to the observed small-scale structure in N_H are given by

$$\alpha_B = \frac{-\ln\langle\exp(-\sigma_B N_H)\rangle}{\sigma_B\langle N_H\rangle} \qquad (3)$$

and

$$\alpha_C = \frac{-\ln\langle\exp(-\sigma_C N_H)\rangle}{\sigma_C\langle N_H\rangle}$$

where the brackets denote an angular average over the $2.^{\circ}5$ (HPBW) Crawford Hill beam size of the enclosed quantity, and σ_B and σ_C are the nominal B and

C band X-ray absorption cross sections, respectively. If the region were mapped with infinite angular resolution, this procedure would measure the actual values of α_B and α_C for this region. Because measurements of finite beamwidth are used, equation (3) provides an estimate of α that is actually an upper limit.

Figure 1 shows histograms of α_B and α_C, calculated for 30 randomly selected regions ($2\overset{\circ}{.}5$ radius) using data from the Hat Creek 21 cm survey (Heiles and Habing 1974, Heiles and Jenkins 1976), which had a beam size of $0\overset{\circ}{.}6$ (HPBW). In all cases, the clumping factor, α, exceeded 0.9 for both the B and C bands, with average values of $\langle\alpha_B\rangle = 0.94$ and $\langle\alpha_C\rangle = 0.97$. Preliminary results from a number of regions the size of the main lobe of the Crawford Hill beam, which were mapped with the 140 foot NRAO telescope (HPBW ~ 20') and corrected for stray radiation by comparison with the Crawford Hill data, give slightly smaller values, with $\alpha_B \gtrsim 0.87$ and $\alpha_C \gtrsim 0.90$ (Jahoda et al. 1984). Similar results are obtained from maps of 500 square degrees made with the 300 foot NRAO telescope at an effective angular resolution of 10'x20' (Verschuur 1974). Searches for significant 21 cm structure on smaller angular scales at intermediate and high latitudes have been uniformly unsuccessful (Dickey 1977; Dickey and Terzian 1978; Lockhart and Goss 1978; Dickey, Salpeter, and Terzian 1979; Dickey 1979; Payne, Salpeter, and Terzian 1982), and we think it unlikely that small-scale structure exists that can reduce α significantly below the values found above. We take $\alpha_B > 0.8$ and $\alpha_C > 0.8$ as conservative estimates of the clumping parameters. However, we have calculated our model count rates for a wide range of values of α.

IV. RESULTS

a) Region near the North Galactic Pole

Figure 2 shows a portion of the scan path near the north galactic pole from flight 25.051, superposed on a map of the Crawford Hill N_H data, which have been interpolated to a 1° grid in right ascension and declination. The directions of the individual data points used in this analysis are shown in Figure 2 and are numbered sequentially. Variations in N_H corresponding to more than an optical depth for C band absorption are present on this portion of the scan path.

The count rate data for these scans are shown in Figure 3. In spite of the large N_H variations in this region, the observed count rates are quite flat. Figure 3 also shows the model predictions for a purely local (unabsorbed) emission model ($I_D = 0$), the solid line, and for a purely distant model ($I_L = 0$, $\alpha = 1.0$), the dashed line. The model with $I_L = 0$ clearly does not fit the data well, whereas the model with $I_D = 0$ is not a bad approximation to the data. Count rates given in the figures are rates predicted for the indicated flights; they do not correspond exactly to the rates on the maps published by McCammon et al (1983), which were normalized to flight 13.103. (Details of the normalizations are given in Burrows (1982).) Fluxes given here are integrated from 0.1 keV to 0.284 keV.

The model of equation (1) was fit to the B band data of flight 25.051 with I_L, I_D, and σ_{eff} as free parameters. Independently, the same model was fit to the C band data. (The minimum values of χ^2 for the B and C band fits were 68.1 and 61.3, respectively, for 61 degrees of freedom, indicating acceptable fits of this model to the data.) Figure 4 shows the 90% and 99% confidence contours for the allowed range of values for I_L and α, which was

defined in equation (2). I_L is given in terms of the count rate for this flight, the emission measure of the local emission region, and the fraction of the total count rate due to the local emission component.

Rather than fitting the model to the B and C band data independently, one would prefer to fit both sets of data simultaneously. That requires a more complicated model. To relate α_B to α_C, some specific clumping geometry of the neutral gas must be assumed. One such picture is discussed in §IVc, but first we emphasize those conclusions which are independent of any such picture.

As discussed in §III, 21 cm observations indicate that a conservative restriction on α is $\alpha>0.8$ for both α_B and α_C. Figure 4 shows that this restriction implies a local fraction of $f_L > 0.69$ for the B band data and $0.56 < f_L < 0.98$ for the C band data at the 99% confidence level for this region of the sky. We note that these local fractions do not conflict with an extrapolation to these energies of the extragalactic power law observed above 2 keV. If the power law continues down to ~0.1 keV, it provides about 1% of the B band count rate in this region and about 8% of the C band count rate. The 99% confidence limits on the emission measures and fluxes of the two emission regions are given in Table 1, with the assumption that $\alpha > 0.8$.

b) Region near the South Galactic Pole

Similar results were found for a region of the same size near the south galactic pole. Figure 5 shows a portion of the scan path of flight 13.049, superposed on a map of the Crawford Hill N_H data, which have been interpolated to a 1° grid in right ascension and declination. The data points used for this analysis are indicated on the figure.

The count rate data for the portions of these scans within 20° of $(284^\circ,-79^\circ)$ are shown in Figure 6, together with the purely local and purely distant model fits to these data. Again, the data are much flatter than predicted under the assumption of distant emission only. The model of equation (1) was fit separately to the B band and C band data, as before. (The minimum χ^2 values, 67.0 and 53.1 for 59 degrees of freedom, again indicate acceptable fits of the model to these data.) Figure 7 shows the 90% and 99% confidence limits for α and I_L for these fits. For $\alpha > 0.8$, these give $f_L > 0.81$ for the B band and $f_L > 0.62$ for the C band at the 99% confidence level. The 99% confidence limits on the intensities of the model components for $\alpha > 0.8$ are given in Table 1.

c) Simultaneous B and C Band Fits

Up to this point our results have been expressed in terms of α_B and α_C as though they were independent quantities. In reality they are related and determined by the geometry of the clumpy structure of the absorbing gas. There is at present no satisfactory model for this clumpiness. One model that is probably as good as any, as far as permitting us to combine our B and C band data is concerned, has all the absorbing gas in randomly distributed clouds of column density N_c. The effect of this kind of clumping on the X-ray absorption cross sections has been discussed by Bowyer and Field (1969) and Bunner et al. (1969). This model gives us

$$\alpha_B = \frac{1}{\sigma_B N_c}\left[1 - \exp(-\sigma_B N_c)\right] \qquad (4)$$

and

$$\alpha_C = \frac{1}{\sigma_C N_c}\left[1 - \exp(-\sigma_C N_c)\right].$$

These equations allow us to simultaneously fit our B and C band data to produce the combined confidence limits shown in Figure 8. Here α_B and α_C are no longer independent parameters, but N_c is free. The combined data allow only a narrow range of values for the intensity of the local component for $\alpha_B > 0.8$. The 25.051 results give limits on the emission measure of the local region of $EM_L \sim 0.0038 \pm 0.0003$ cm^{-6} pc (99% confidence). This implies that $I_L = 49 \pm 3$ cps for the B band and $I_L = 200 \pm 10$ cps for the C band. The local emission measure in this region is more than a factor of 2 larger than the emission measure required in the galactic plane (~ 0.0017 cm^{-6} pc).

The results for 13.049 are similar, with $EM_L \sim 0.0028 \pm 0.0002$ cm^{-6} pc for $\alpha > 0.8$ (99% confidence). This gives $I_L = 41 \pm 3$ cps for the B band and $I_L = 140 \pm 10$ cps for the C band. Again, this is substantially higher than the intensity observed in the galactic plane. These results imply that the local component, which contributes most of the observed count rate in both regions, is anisotropic on large angular scales.

V. DISCUSSION AND CONCLUSIONS

Our strongest upper limit on the emission measure of hot gas outside the galactic neutral gas is $EM_D < 0.0017$ cm^{-6} pc, which implies an upper limit on the unabsorbed distant intensity of 1.2×10^{-8} ergs cm^{-2} s^{-1} sr^{-1} (0.1-0.284 keV) at the 99% confidence limit. The corresponding upper limit from a previous measurement of soft diffuse X-rays from the direction of the Small Magellanic Cloud was 2.6×10^{-8} ergs cm^{-2} s^{-1} sr^{-1} (McCammon et al. 1976). We emphasize that this limit applies to X-ray emission originating beyond all of the neutral gas with velocity in the range -100 to +100 km s^{-1}.

As was stated earlier, the two spatial regions considered in the paragraphs above (§IVa,b and c) were chosen for detailed analysis because they provided good quality X-ray data in relatively small regions near the north and south galactic poles. Quite apart from these detailed analyses, even a qualitative perusal of Figures 5 and 6 shows that there is, in these small regions, no convincing tendency for the X-ray intensity to decrease in directions where significant absorption is predicted. On a global scale, however, there is a long-established anticorrelation between X-ray intensity and column density of absorbing gas. There must be X-ray intensity features more nearly consistent with absorption in some spatial regions. In fact, when the remainder of the scans near the SGP are examined, absorption-like features are evident.

The scans beyond 20° from (284°,-79°) cross a sharp gradient in N_H and a roughly circular cloud-like feature approximately 10° in diameter (see Fig. 5). Figure 9 shows the observed count rates from all points within 35° of (284°,-79°), together with predictions for purely local and purely

distant emission. Counting rates tend to be low around observation points 40, 65 and 90 where significant absorption is predicted. On the other hand, even though the rates are roughly constant during observations 1 to 30, significant absorption centered on point 12 is predicted.

We suggest that the real disposition of hot emitting and cold absorbing gas is considerably more complicated than described by equation (1). If there is significant distant emission from an extragalactic source or from an extended halo, all features in the absorbing gas must be accompanied by X-ray absorption. We have shown this not to be the case. On the other hand, a global anticorrelation of soft X-ray intensity and H I column density does exist, and in the paragraph above we have pointed to a specific region where there seem to be intensity features at least suggestive of absorption. Perhaps the essential oversimplification of the model described by equation (1) is the separation of emission into just two components: one local and unabsorbed, one distant and absorbed. This is probably too naive, in light of recent evidence for the existence of neutral gas at more than 1 kpc above the galatic plane (Hobbs et al. 1982, Lockman 1984, Albert 1983). Our knowledge of the structure of the interstellar medium is certainly unsettled enough to allow alternate regions of hot emitting and cold absorbing gas of various thicknesses (Hayakawa 1979) above and below as well as in the galactic plane. A feature in the column density of cold neutral gas can result then, under a model of this type, in widely different depths of absorption. It all depends upon where along the line of sight the gas responsible for the column density feature is located.

The analysis we have presented was undertaken in order to set an upper limit on the amount of soft X-ray emission that originates on the far side of the neutral galactic gas. The upper bound results of ξ_{IV} remain valid even if emission and absorption are mixed, for under the simple model described by equation (1), all absorption features are attributed to distant emission, whereas in a mixed emission-absorption model some neutral hydrogen may be beyond the emitting gas. Therefore, we hesitate to associate "distant emission" with "halo emission", for it seems quite possible that there is hot halo gas on the near side of some of the neutral absorbing gas.

We are grateful to Carl Heiles for sending us the Crawford-Hill 21 cm profiles prior to publication. This work was supported by NASA grant NGL 50-002-044.

REFERENCES

Albert, C. E. 1983, Ap. J., 272, 509.

Bowyer, C. S., and Field, G. B. 1969, Nature, 223, 573.

Bowyer, C. S., Field, G. B., and Mack, J. E. 1968, Nature, 217, 32.

Bregman, J. N. 1980a, Ap. J., 236, 577.

Bregman, J. N. 1980b, Ap. J., 237, 681.

Bregman, J. N., and Glassgold, A. E. 1982, Ap. J., 263, 564.

Brown, R. L., and Gould, R. J. 1970, Phys. Rev. D, 1, 2252.

Bunner, A. N., Coleman, P. L., Kraushaar, W. L., McCammon, D., Palmieri, T. M., Shilepsky, A., and Ulmer, M. 1969, Nature, 223, 1222.

Burrows, D. N. 1982, Ph.D. thesis, University of Wisconsin, Madison.

Chevalier, R. A., and Oegerle, W. R. 1979, Ap. J., 227, 398.

Cox, D. P. 1981, Ap. J., 245, 534.

Cox, D. P., and Anderson, P. R. 1982, Ap. J., 253, 268.

Dickey, J. M. 1977, Ph.D. thesis, Cornell University.

Dickey, J. M. 1979, Ap. J., 233, 558.

Dickey, J. M., Salpeter, E. E., and Terzian, Y. 1978, Ap. J. Suppl., 36, 77.

Dickey, J. M., Salpeter, E. E., and Terzian, Y. 1979, Ap. J., 228, 465.

Hayakawa, S. 1979, in (COSPAR) X-ray Astronomy, eds. W. A. Baity and L. E. Peterson (Oxford: Pergammon), 323.

Heiles, C., and Habing, H. J. 1974, Astr. Ap. Suppl., 14, 1.

Heiles, C., and Jenkins, E. B. 1976, Astr. Ap., 46, 333.

Hobbs, L. M., Morgan, W. W., Albert, C. E., and Lockman, F. J. 1982, Ap. J., 263, 690.

Jahoda, K. M., McCammon, D., Dickey, J. M., and Lockman, F. J. 1984, in preparation.

Jenkins, E. B. 1978a, Ap. J., 219, 845.

———. 1978b, Ap. J., 220, 107.

Jenkins, E. B., and Meloy, D. A. 1974, Ap. J. (Letters), 193, L121.

Lampton, M., Margon, B., and Bowyer, S. 1976, Ap. J., 208, 177.

Levine, A., Rappaport, S., Halpern, J., and Walter, F. 1977, Ap. J., 211, 215.

Lockhart, I. A., and Goss, W. M. 1978, Astr. Ap., 67, 355.

Lockman, F. J. 1984, "HI Halo Inner Galaxy", preprint.

Long, K. S., Agrawal, P. C., and Garmire, G. P. 1976, Ap. J., 206, 411.

McCammon, D., Bunner, A. N., Coleman, P. L., and Kraushaar, W. L. 1971, Ap. J. (Letters), 168, L33.

McCammon, D., Burrows, D. N., Sanders, W. T., and Kraushaar, W. L. 1983, Ap. J., 269, 107.

McCammon, D., Meyer, S. S., Sanders, W. T., and Williamson, F. O. 1976, Ap. J., 209, 46.

McKee, C. F., and Ostriker, J. P. 1977, Ap. J., 218, 148.

Payne, H. E., Salpeter, E. E., and Terzian, Y. 1982, Ap. J. Suppl., 48, 199.

Penzias, A. A., Wilson, R. W., and Encrenaz, P. J. 1970, A. J., 75, 141.

Raymond, J. C., and Smith, B. W. 1977, Ap. J. Suppl., 35, 419.

———. 1979, private communication (update to Raymond and Smith 1977).

Rosner, R., Avni, Y., Bookbinder, J., Giaconni, R., Golub, L., Harnden, F. R. Jr., Maxson, C. W., Topka, K., and Vaiana, G. S. 1981, Ap. J. (Letters), 249, L5.

Shapiro, P. R., and Field, G. B. 1976, Ap. J., 205, 762.

Stark, A. A., Heiles, C., Bally, J., and Linke, R. 1984, in preparation.

Vanderhill, M. J., Borken, R. J., Bunner, A. N., Burstein, P. H., and Kraushaar, W. L. 1975, Ap. J. (Letters), 197, L19.

Verschuur, G. L. 1974, Ap. J. Suppl., 27, 65.

Williamson, F. O., Sanders, W. T., Kraushaar, W. L., McCammon, D., Borken, R., and Bunner, A. N. 1974, Ap. J. (Letters), 193, L133.

Author's Addresses

D. N. Burrows, Department of Astronomy, Pennsylvania State University, 525 Davey Laboratory, University Park, PA 16802

D. McCammon, W. T. Sanders and W. L. Kraushaar, Department of Physics, University of Wisconsin, Madison, WI 53711

TABLE 1

99% Confidence Limits (for $\alpha > 0.8$)

	Flight 25.051 (log T = 6.00)			Flight 13.049 (log T = 6.05)		
Energy Band	B	C	B + C	B	C	B + C
Local emission measure, EM_L (cm^{-6} pc)	0.0041> EM_L>0.0028	0.0040> EM_L>0.0023	0.0041> EM_L>0.0035	0.0030> EM_L>0.0025	0.0030> EM_L>0.0019	0.0030> EM_L>0.0026
Flux from local region, F_L, 0.1-0.28 keV (ergs cm^{-2} s^{-1} sr^{-1})	3.1×10^{-8}> F_L>2.2×10^{-8}	3.1×10^{-8}> F_L>1.8×10^{-8}	3.1×10^{-8}> F_L>2.7×10^{-8}	2.2×10^{-8}> F_L>1.8×10^{-8}	2.2×10^{-8}> F_L>1.4×10^{-8}	2.2×10^{-8}> F_L>1.9×10^{-9}
Distant emission measure, EM_D (cm^{-6} pc)	EM_D<0.0175	0.0007<EM_D<0.0072	EM_D<0.0029	EM_D<0.0058	EM_D<0.0044	EM_D<0.0017
Flux from distant region,[a] F_D, 0.1-0.28 keV (ergs cm^{-2} s^{-1} sr^{-1})	F_D<1.3×10^{-7}	5.3×10^{-9}< F_D<5.5×10^{-8}	F_D<2.2×10^{-8}	F_D<4.2×10^{-8}	F_D<3.2×10^{-8}	F_D<1.2×10^{-8}

[a]Flux from an extrapolation of the power law observed above 2 keV is 6.4×10^{-9} ergs cm^{-2} s^{-1} sr^{-1}.

Figure Captions

Fig. 1.- Values of the clumping parameter, α, found by applying eqn. (3) to high latitude data from the Hat Creek 21 cm survey. The clumping parameter was calculated for randomly selected directions with $|b| > 20^\circ$. For each direction, α_B and α_C were calculated for a field $2\overset{\circ}{.}5$ in radius centered on that direction. This calculation of α provides a measure of the reduction in the effective X-ray absorption cross section caused by structure in the H I column densities on angular scales between the resolution of the Hat Creek survey ($0\overset{\circ}{.}6$ HPBW) and that of the Crawford Hill survey ($2\overset{\circ}{.}5$ HPBW). (a) α_B, the clumping parameter for the B band. (b) α_C, the clumping parameter for the C band.

Fig. 2.- Scan path of flight 25.051, superposed on the N_H map made from the Crawford Hill data, which were interpolated to 1° in right ascension and declination. The contour interval is 5×10^{19} cm^{-2}. Only points within 20° of $(\ell,b) = (215^\circ,85^\circ)$ are included in the plot or the analysis. The data points are labeled in sequential order.

Fig. 3.- B and C band count rates for the region shown in Fig. 2. (a) The observed B band count rate of each data point is shown with the 1σ error bars expected from counting statistics. The heavy solid line indicates the model prediction for an isotropic emission region absorbed only by the Earth's atmosphere. The dashed line indicates the model prediction for an isotropic emission region located beyond all the neutral gas of the galactic disk. (b) Same as Fig. 3a, but for the C band.

Fig. 4.- Confidence limits on the clumping parameters, α_B and α_C, and the intensity of the local emission component. The latter is given in terms of the fraction of the observed count rate originating in the local emission

region, the count rate due to the local emission region (I_L), and the emission measure of the local region (EM_L). The count rates given here are for flight 25.051, and are not normalized to the all-sky maps presented in McCammon et al. (1983). (a) Confidence limits from the B band data. (b) Confidence limits from the C band data.

Fig. 5.- Same as Fig. 2, but for flight 13.049. Points within 35° of $(\ell,b) = (284^\circ,-79^\circ)$ are shown.

Fig. 6.- Same as Fig. 3, but for flight 13.049. Only points within 20° of $(284^\circ,-79^\circ)$ are included in this figure.

Fig. 7.- Same as Fig. 4, but for flight 13.049.

Fig. 8.- Combined B and C band confidence limits. The B and C band clumping parameters were related to each other by means of a model of the assumed clumping. This figure assumes the clumping model discussed in the text and embodied in eqn. (4). A different clumping model would result in different confidence limits for this figure. (a) Confidence limits for the region scanned by 25.051. (b) Confidence limits for the region scanned by 13.049.

Fig. 9.- Same as Fig. 6, but for data points within 35° of $(284^\circ,-79^\circ)$.

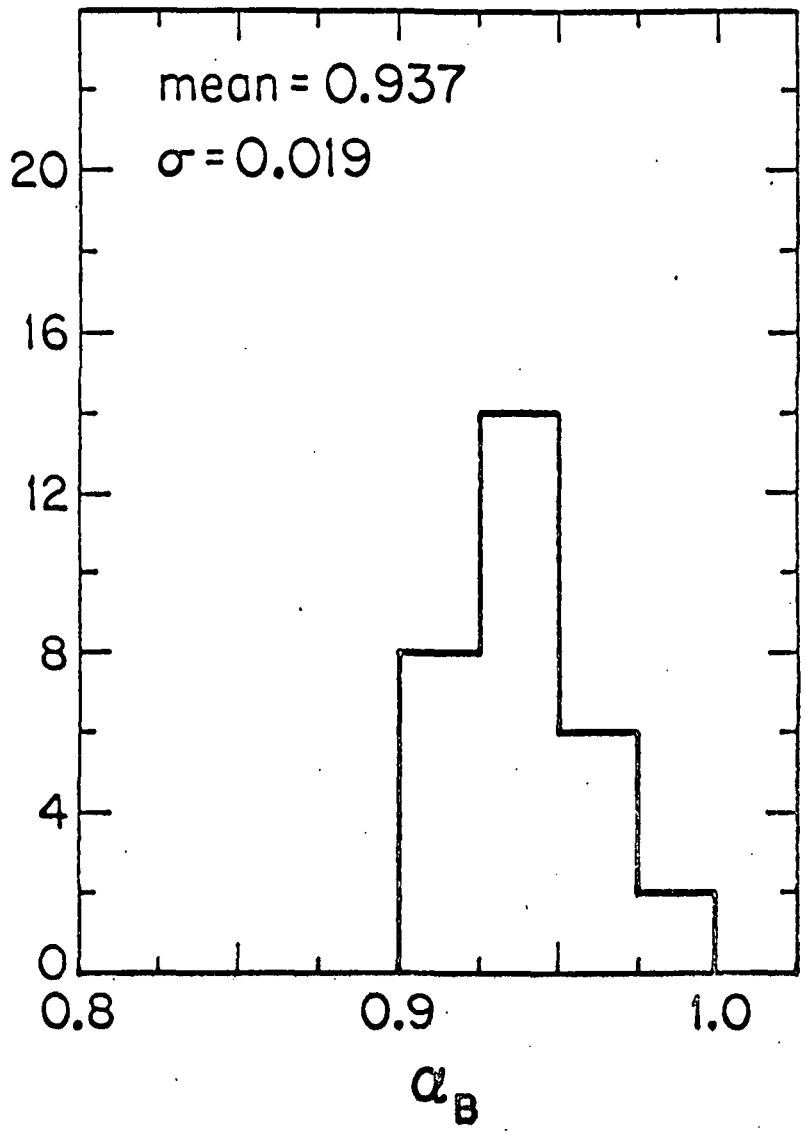
mean = 0.937
σ = 0.019
20
16
12
8
4
0
0.8
0.9
1.0
α_B

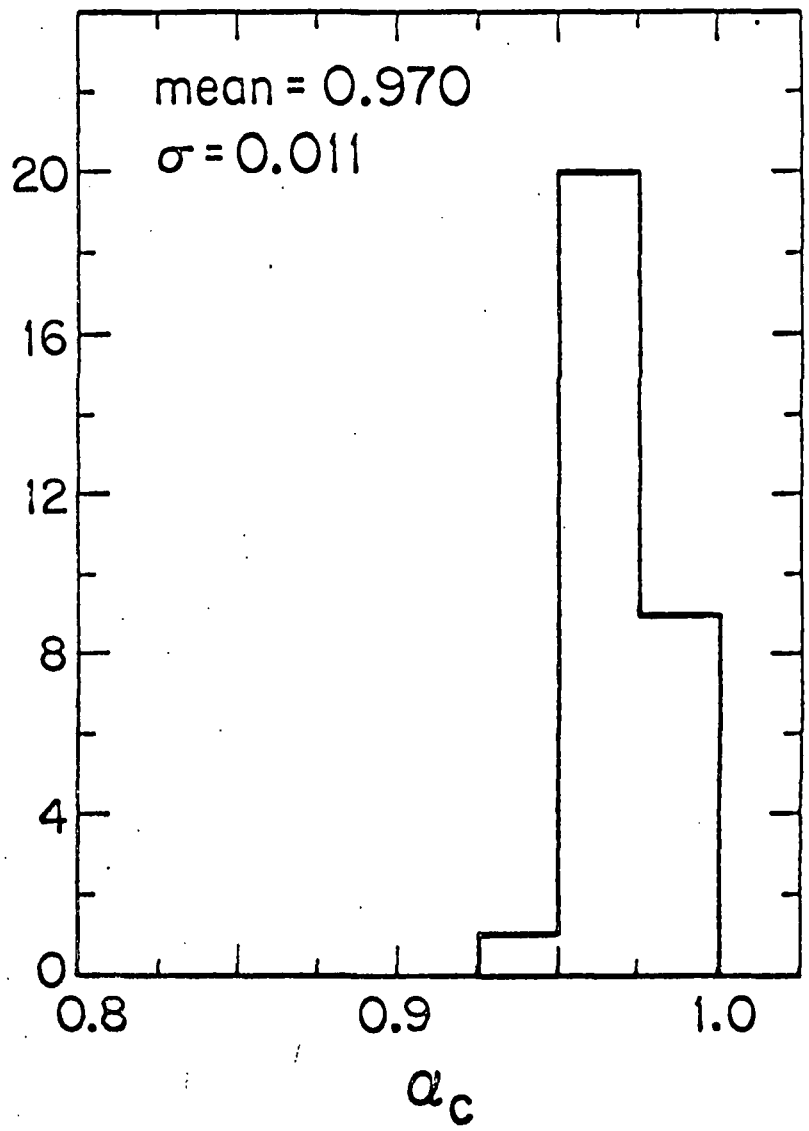
mean = 0.970
σ = 0.011
20
16
12
8
4
0
0.8
0.9
1.0
α_C

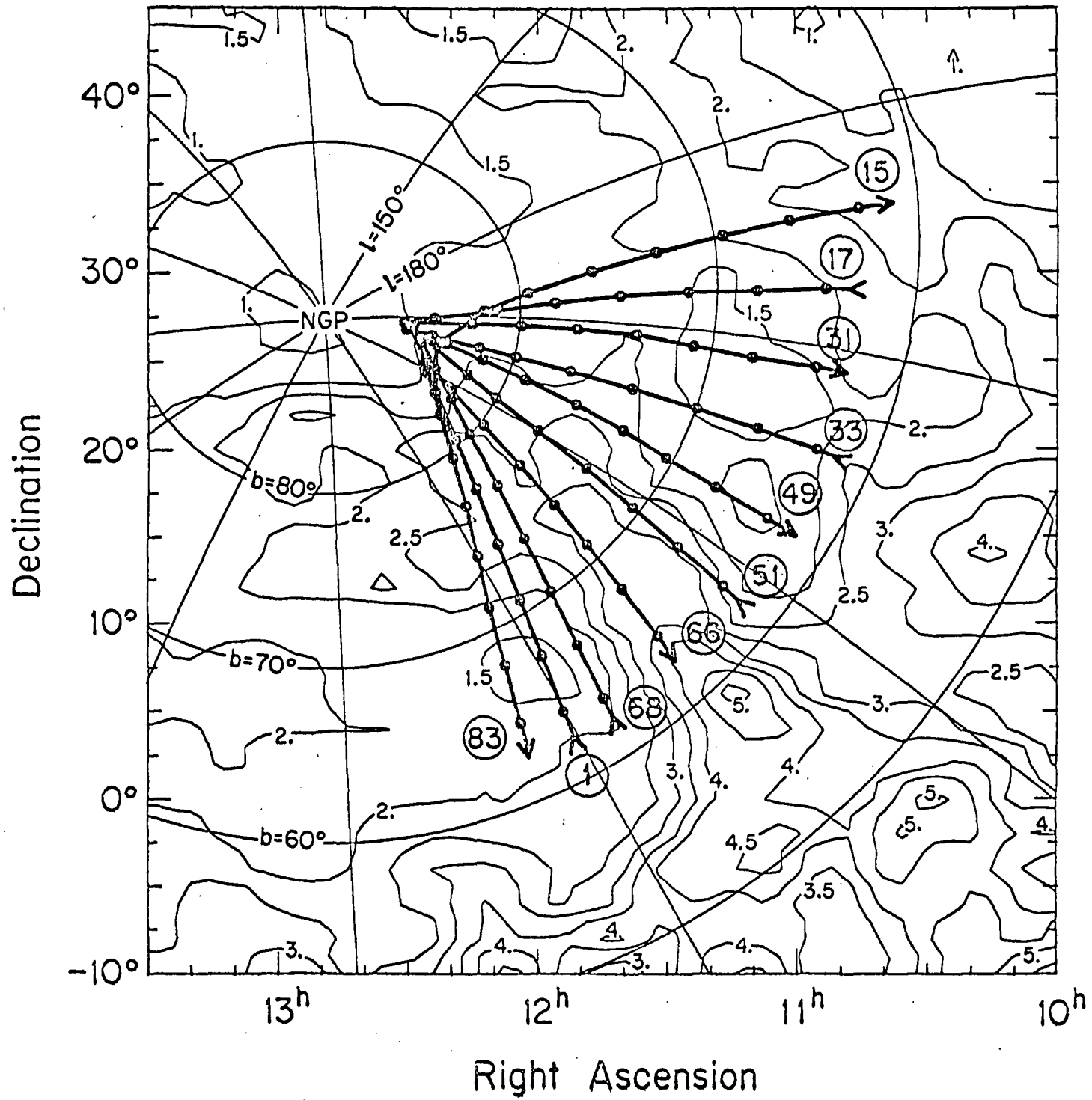
Declination
Right Ascension
40°
30°
20°
10°
0°
-10°
13h
12h
11h
10h
NGP
l=150°
l=180°
b=80°
b=70°
b=60°
15
17
31
33
49
51
66
68
83
1
1.
1.5
2.
2.5
3.
4.
4.5
5.
3.5

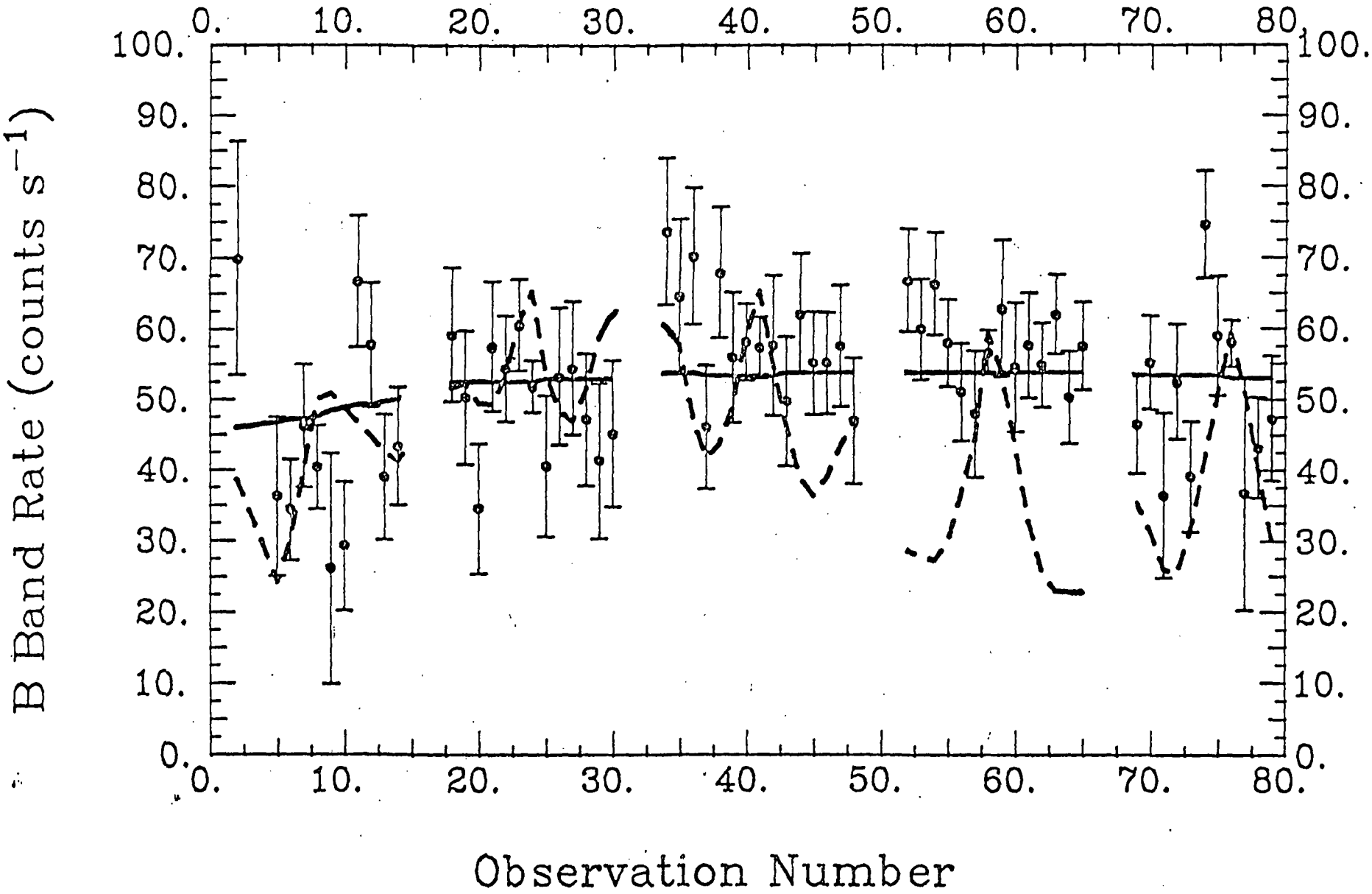
25.051 SCANS WITH B > 65 DEGREES
B Band Rate (counts s^{-1})
Observation Number
0.
10.
20.
30.
40.
50.
60.
70.
80.
90.
100.

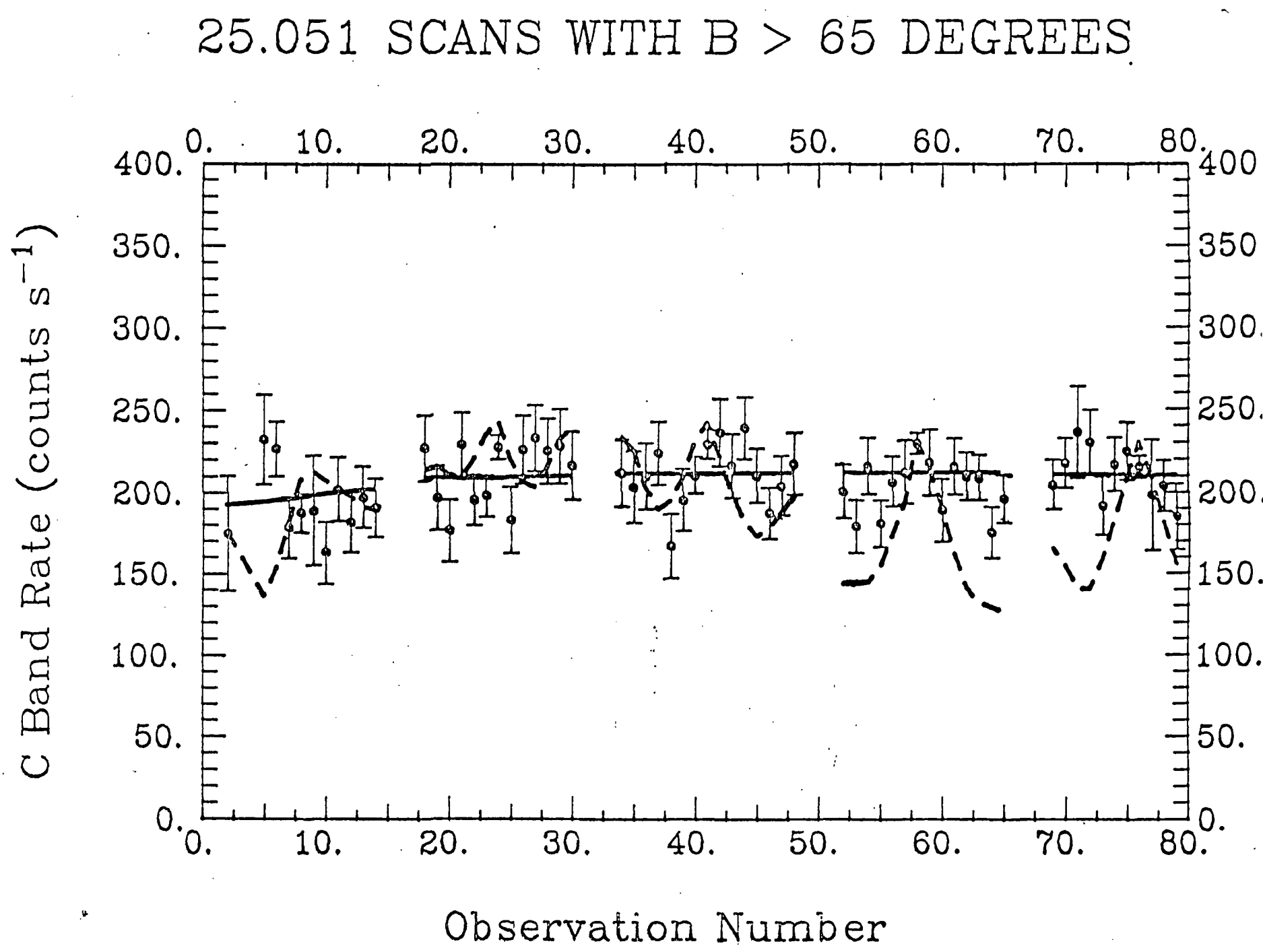
25.051 SCANS WITH B > 65 DEGREES
C Band Rate (counts s^{-1})
Observation Number
0.
50.
100.
150.
200.
250.
300.
350.
400.
10.
20.
30.
40.
50.
60.
70.
80.

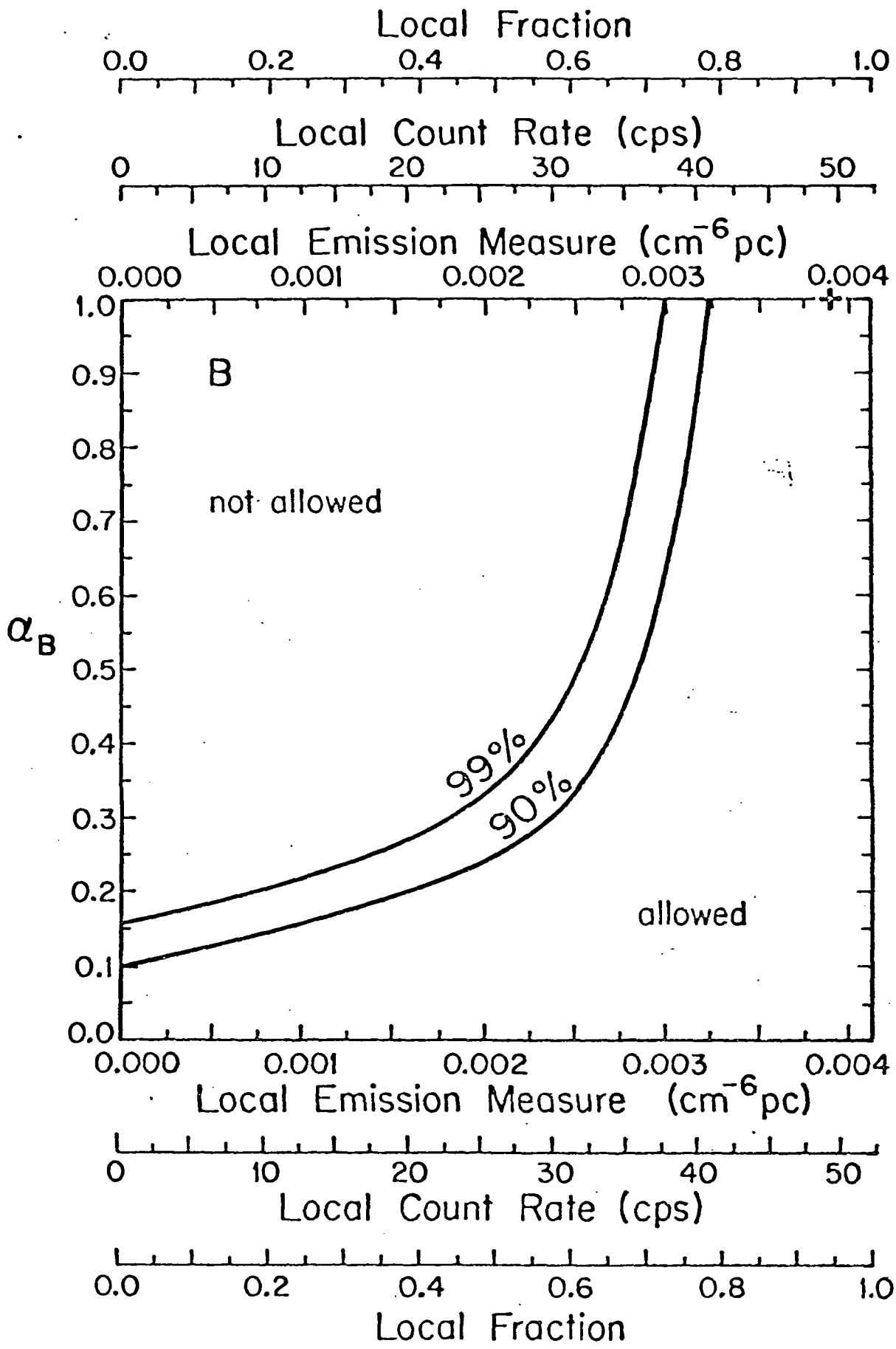
Local Fraction
0.0
0.2
0.4
0.6
0.8
1.0
Local Count Rate (cps)
0
10
20
30
40
50
Local Emission Measure (cm^{-6}pc)
0.000
0.001
0.002
0.003
0.004
B
not allowed
α_B
99%
90%
allowed

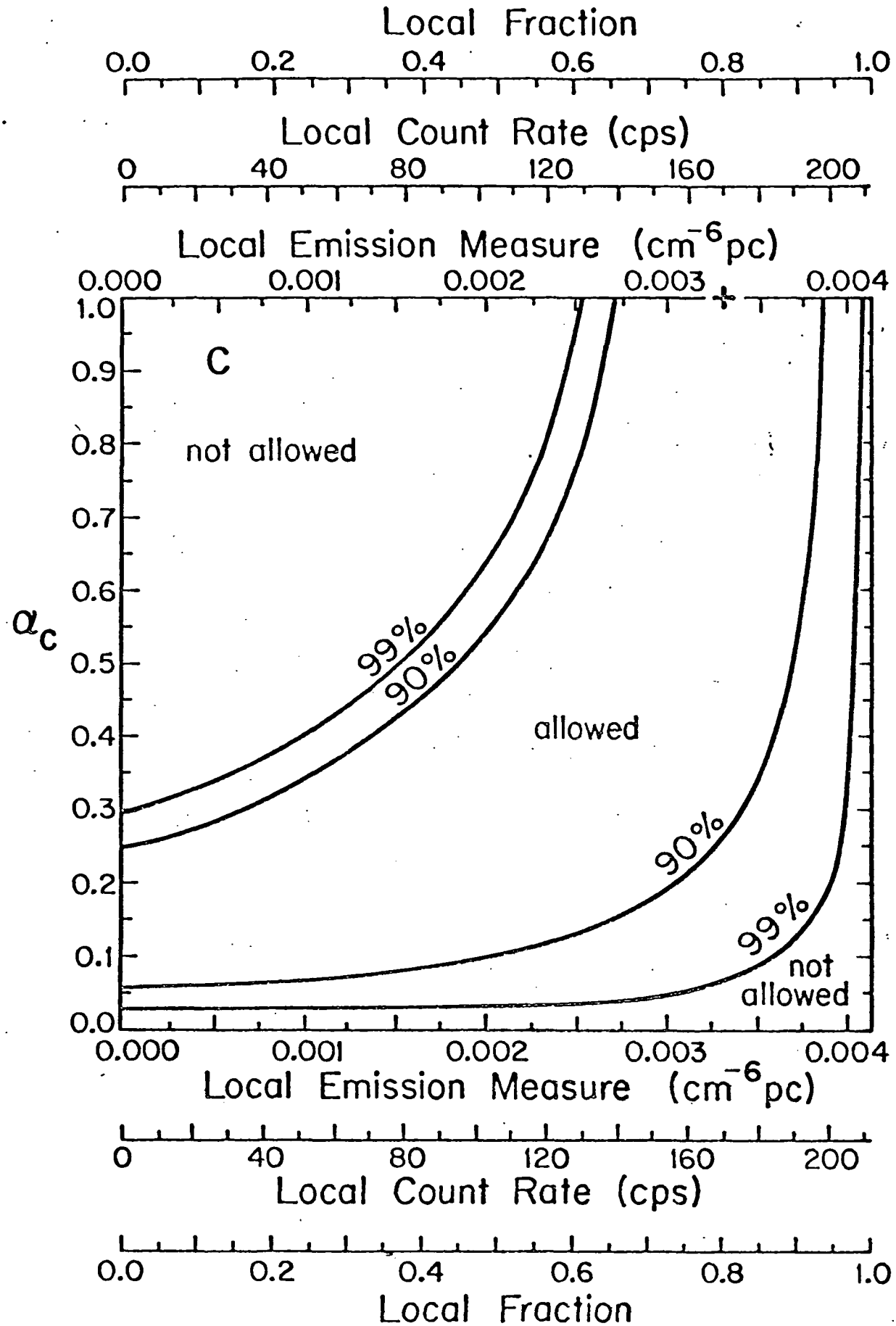
Local Fraction
0.0
0.2
0.4
0.6
0.8
1.0
Local Count Rate (cps)
0
40
80
120
160
200
Local Emission Measure (cm⁻⁶pc)
0.000
0.001
0.002
0.003
0.004
C
not allowed
99%
90%
allowed
90%
99%
not allowed
α_c
1.0
0.9
0.8
0.7
0.6
0.5
0.4
0.3
0.2
0.1
0.0

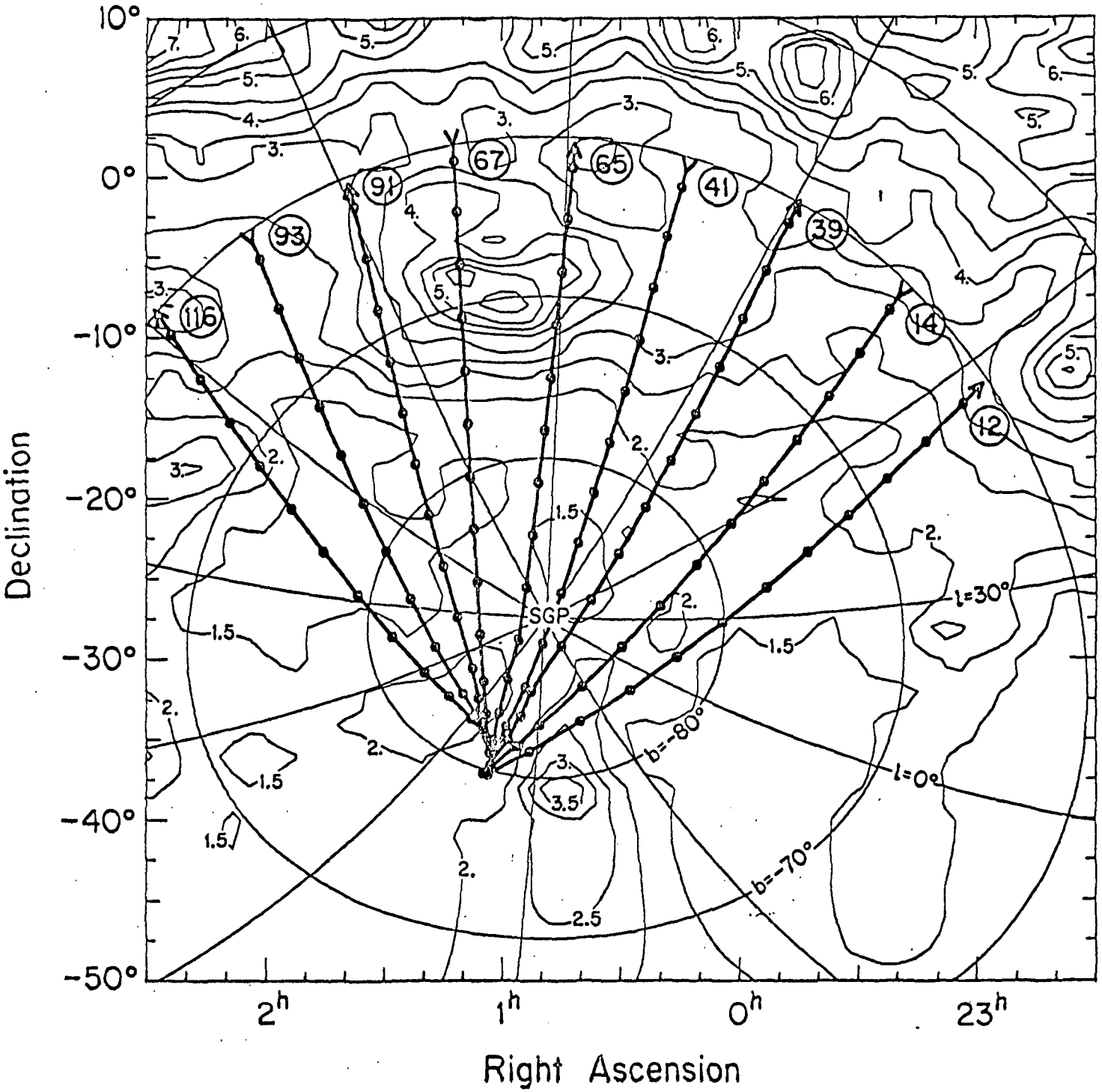
10°
0°
-10°
-20°
-30°
-40°
-50°
Declination
2h
1h
0h
23h
Right Ascension
SGP
l=30°
l=0°
b=-80°
b=-70°
67
65
91
41
93
39
116
14
12
1
7.
6.
5.
4.
3.
2.
1.5
3.5
2.5

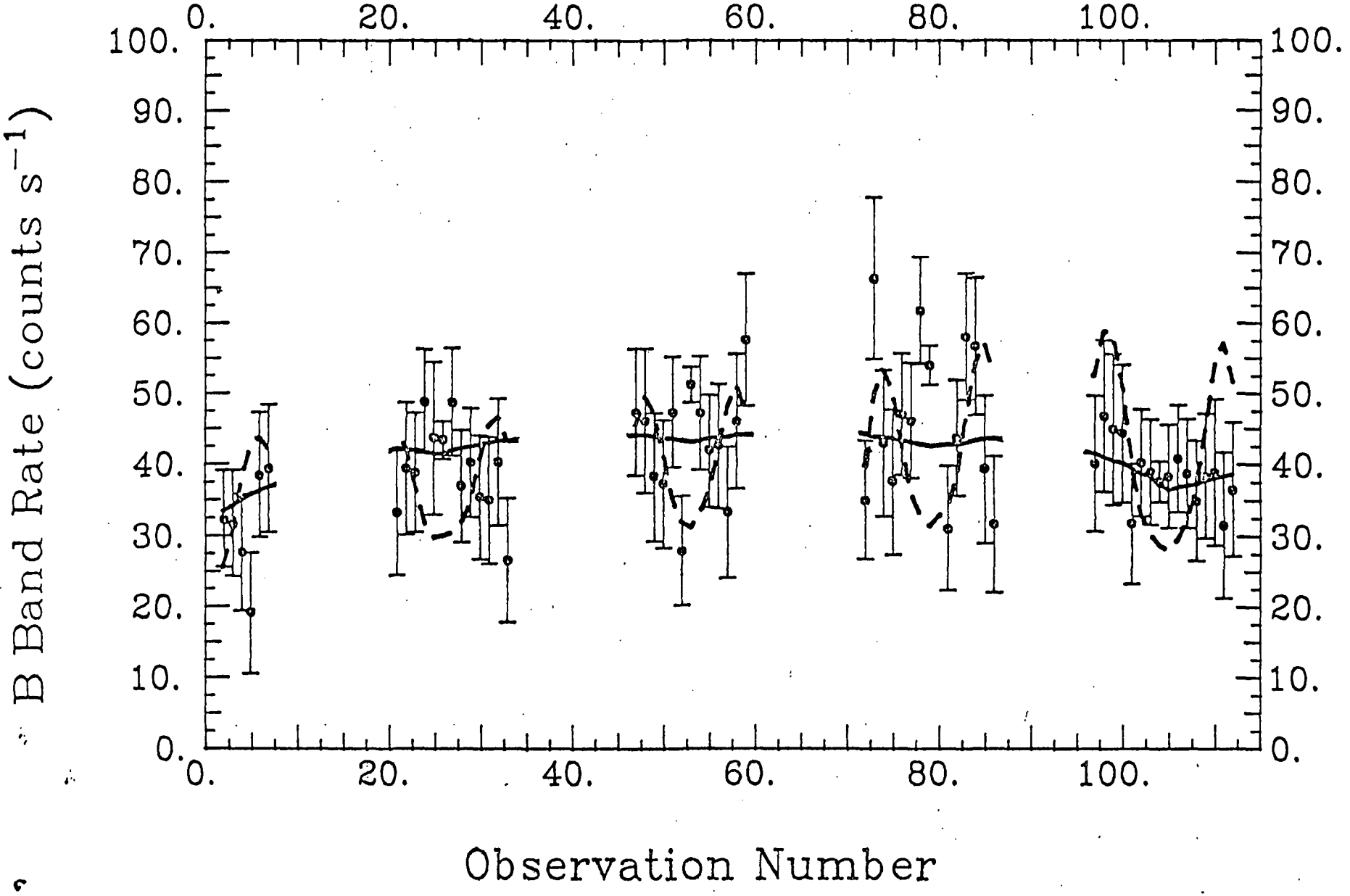
13.049 SCANS WITHIN 20 DEGREES OF PITCH POINT
B Band Rate (counts s^{-1})
Observation Number
0.
20.
40.
60.
80.
100.
10.
30.
50.
70.
90.

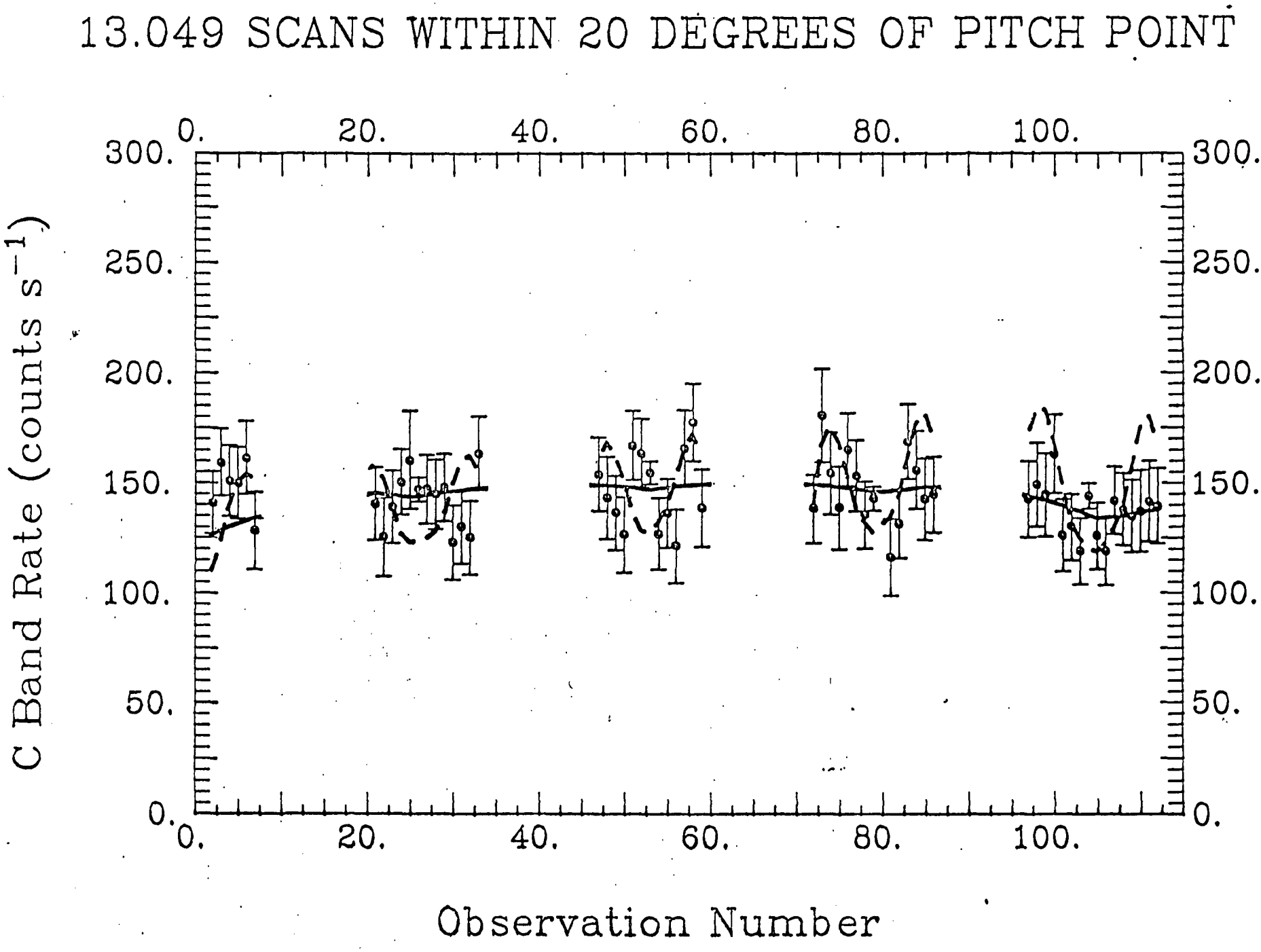
13.049 SCANS WITHIN 20 DEGREES OF PITCH POINT
C Band Rate (counts s^{-1})
Observation Number
0.
20.
40.
60.
80.
100.
300.
250.
200.
150.
100.
50.
0.

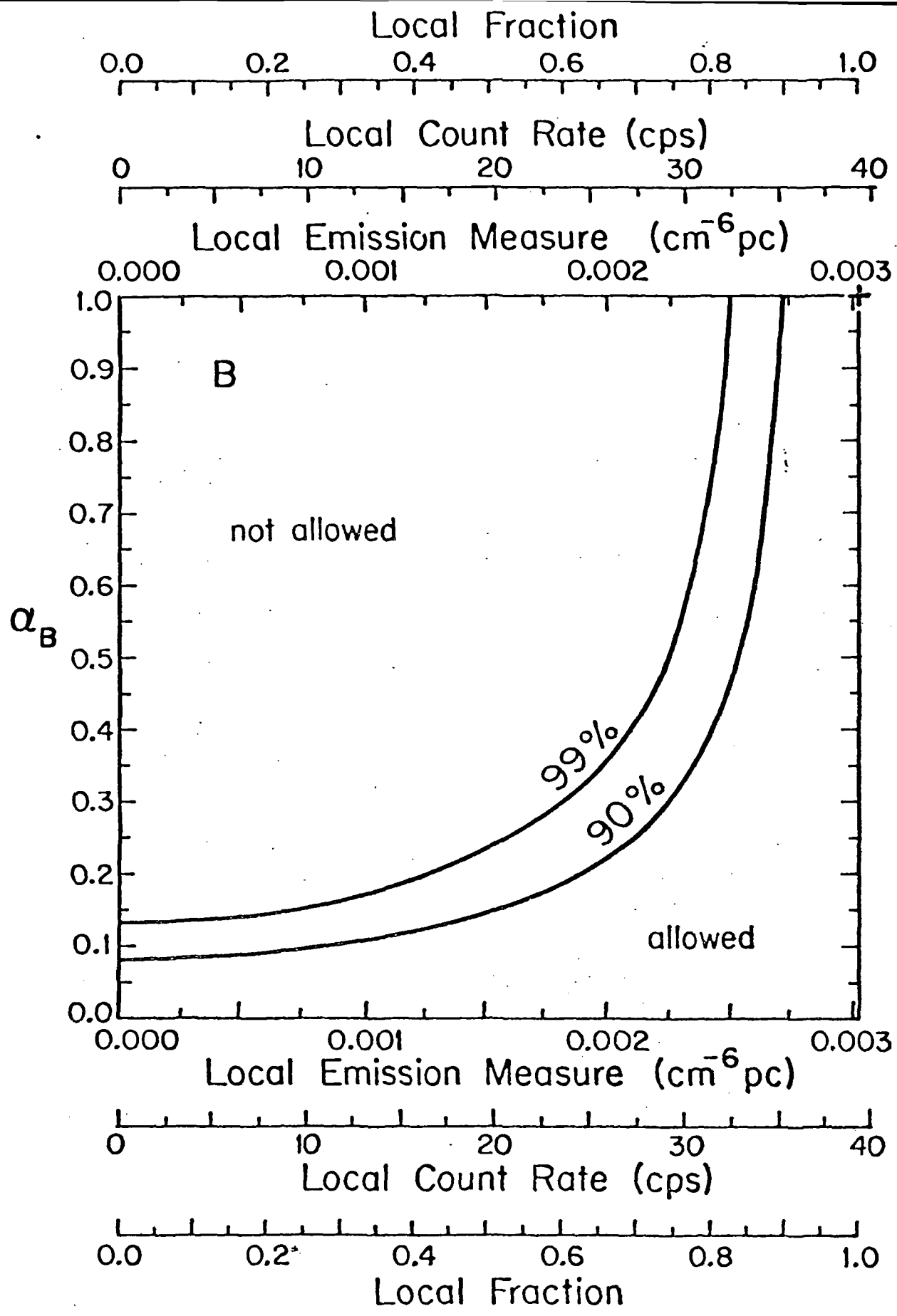
Local Fraction
0.0
0.2
0.4
0.6
0.8
1.0
Local Count Rate (cps)
0
10
20
30
40
Local Emission Measure (cm⁻⁶pc)
0.000
0.001
0.002
0.003
B
not allowed
99%
90%
allowed
α_B
0.0
0.1
0.2
0.3
0.4
0.5
0.6
0.7
0.8
0.9
1.0

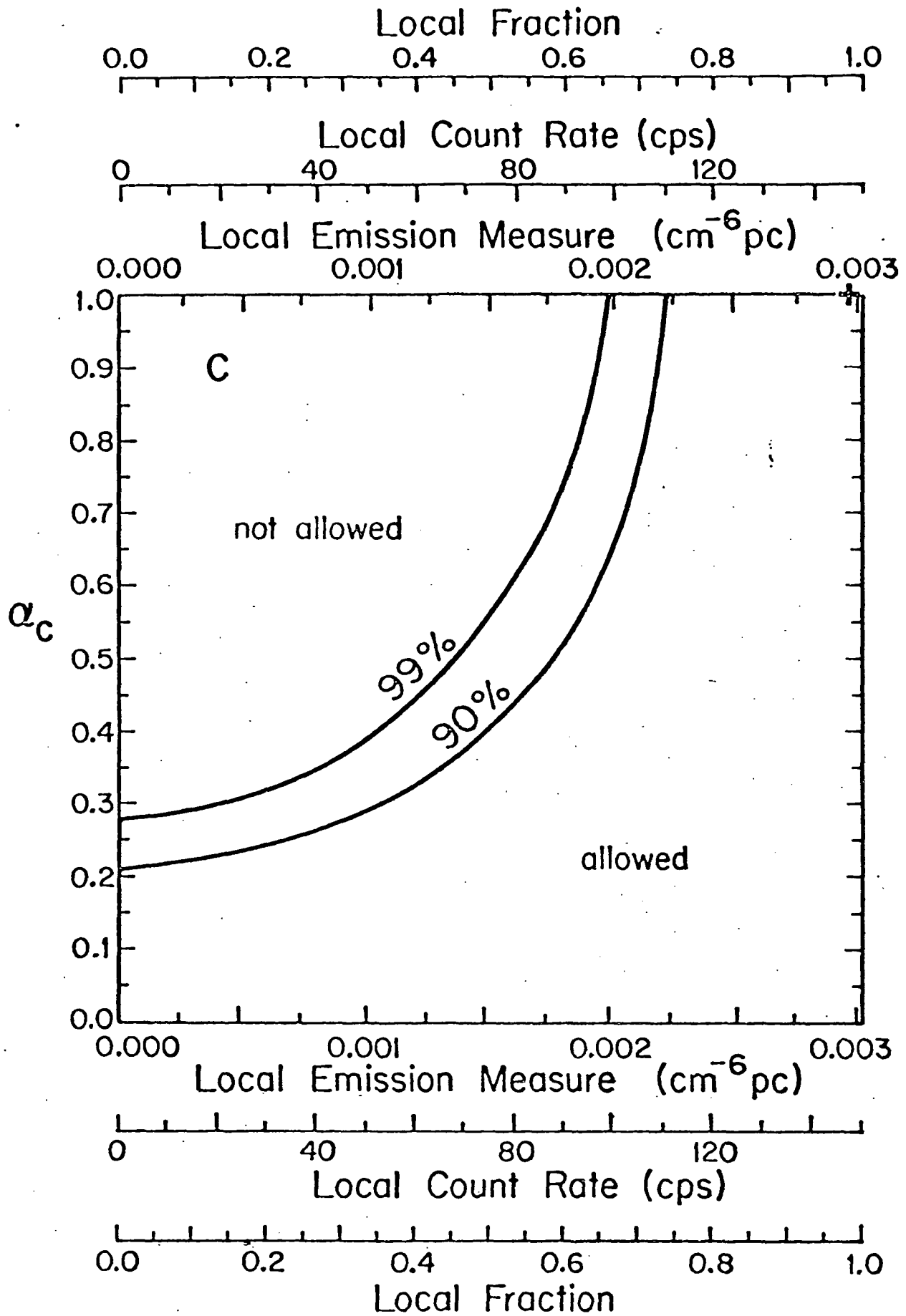
Local Fraction
0.0
0.2
0.4
0.6
0.8
1.0
Local Count Rate (cps)
0
40
80
120
Local Emission Measure (cm^{-6}pc)
0.000
0.001
0.002
0.003
C
not allowed
99%
90%
allowed
α_c
1.0
0.9
0.8
0.7
0.6
0.5
0.4
0.3
0.2
0.1
0.0

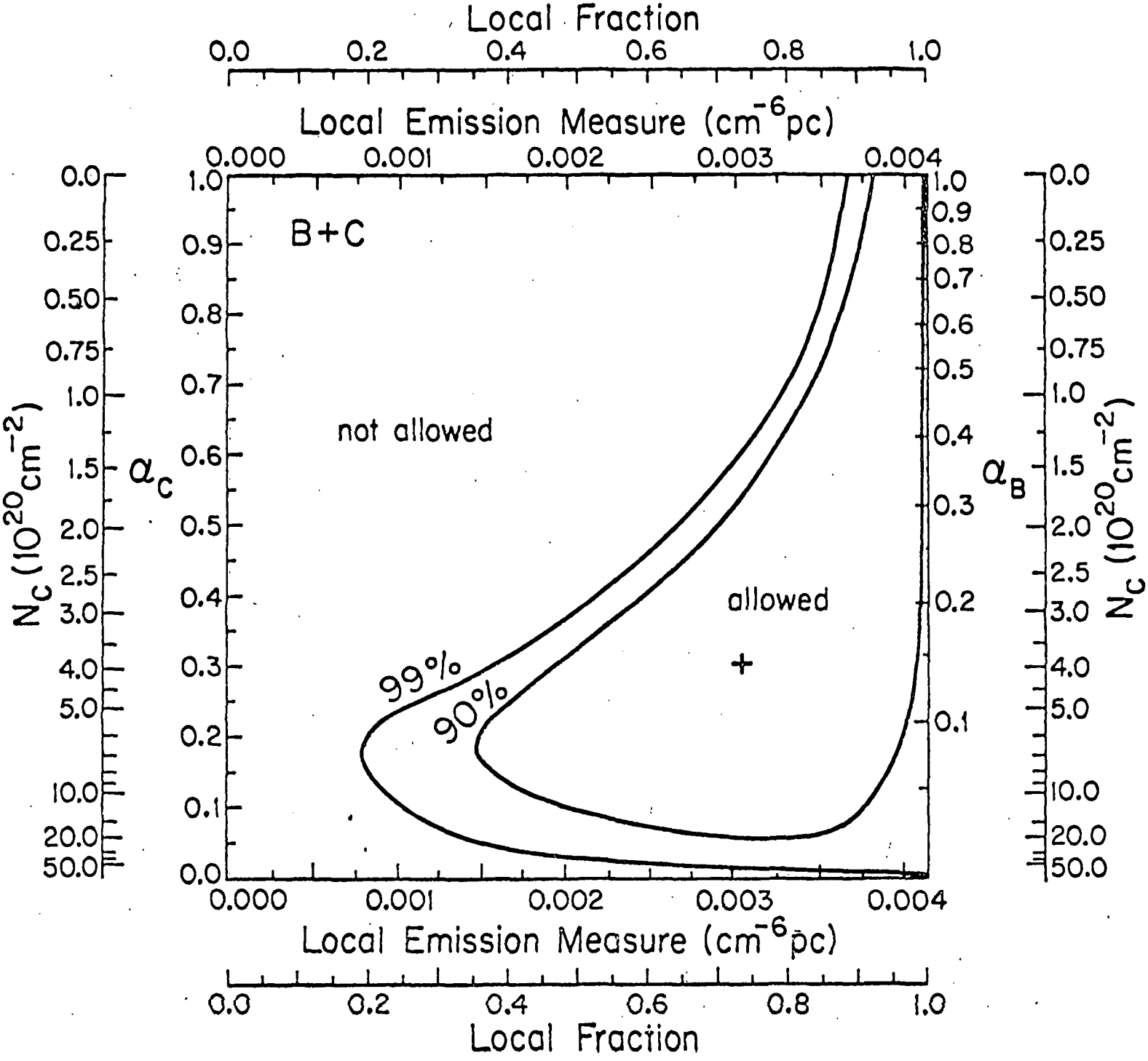
Local Fraction
0.0
0.2
0.4
0.6
0.8
1.0
Local Emission Measure (cm^{-6}pc)
0.000
0.001
0.002
0.003
0.004
B+C
not allowed
allowed
99%
90%
α_C
α_B
N_C (10^{20}cm^{-2})
0.0
0.25
0.50
0.75
1.0
1.5
2.0
2.5
3.0
4.0
5.0
10.0
20.0
50.0
1.0
0.9
0.8
0.7
0.6
0.5
0.4
0.3
0.2
0.1
0.0

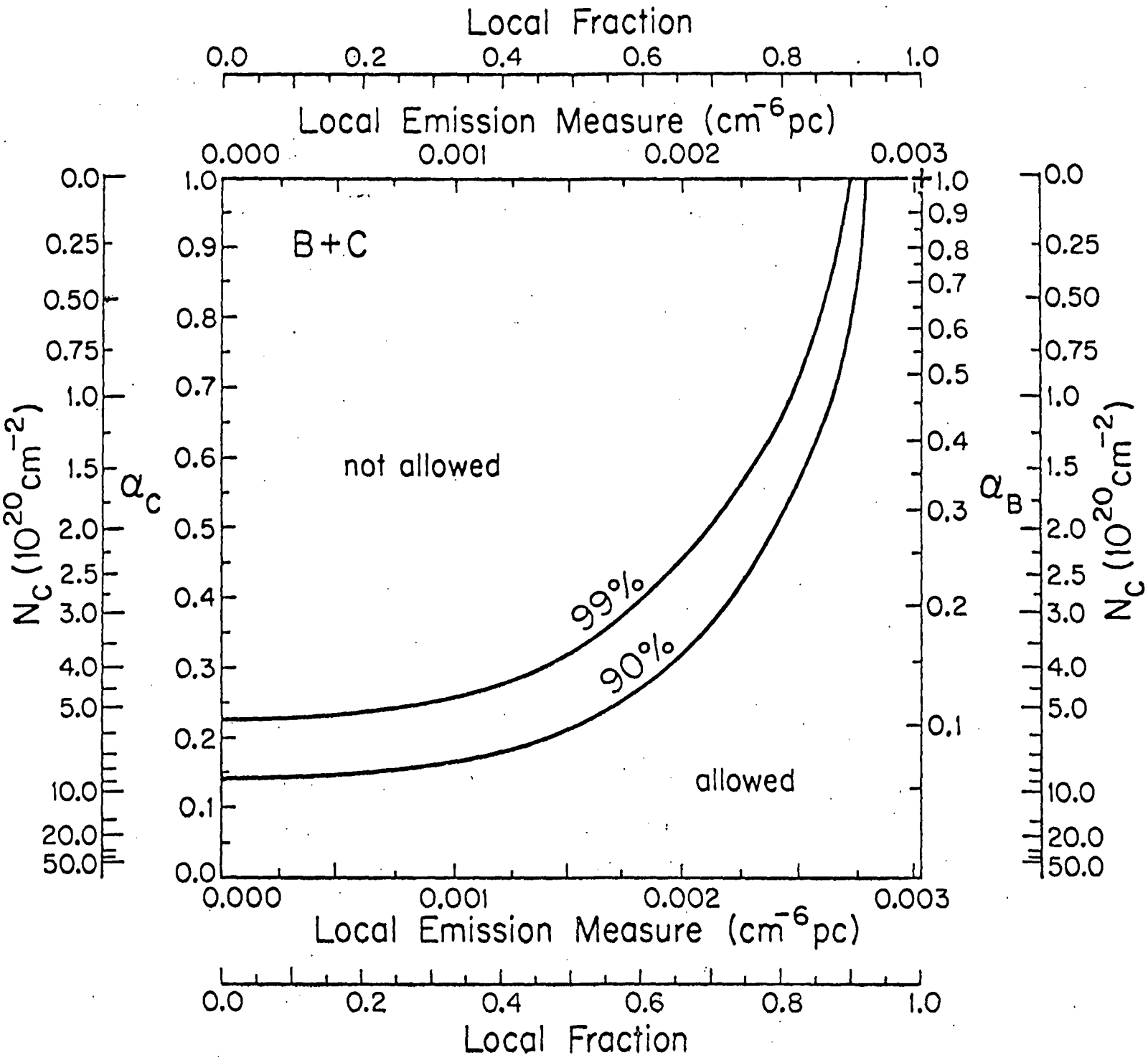
Local Fraction
0.0
0.2
0.4
0.6
0.8
1.0
Local Emission Measure ($cm^{-6}pc$)
0.000
0.001
0.002
0.003
B+C
not allowed
allowed
99%
90%
N_C ($10^{20}cm^{-2}$)
α_C
α_B
0.0
0.25
0.50
0.75
1.0
1.5
2.0
2.5
3.0
4.0
5.0
10.0
20.0
50.0
0.9
0.8
0.7
0.6
0.5
0.4
0.3
0.2
0.1

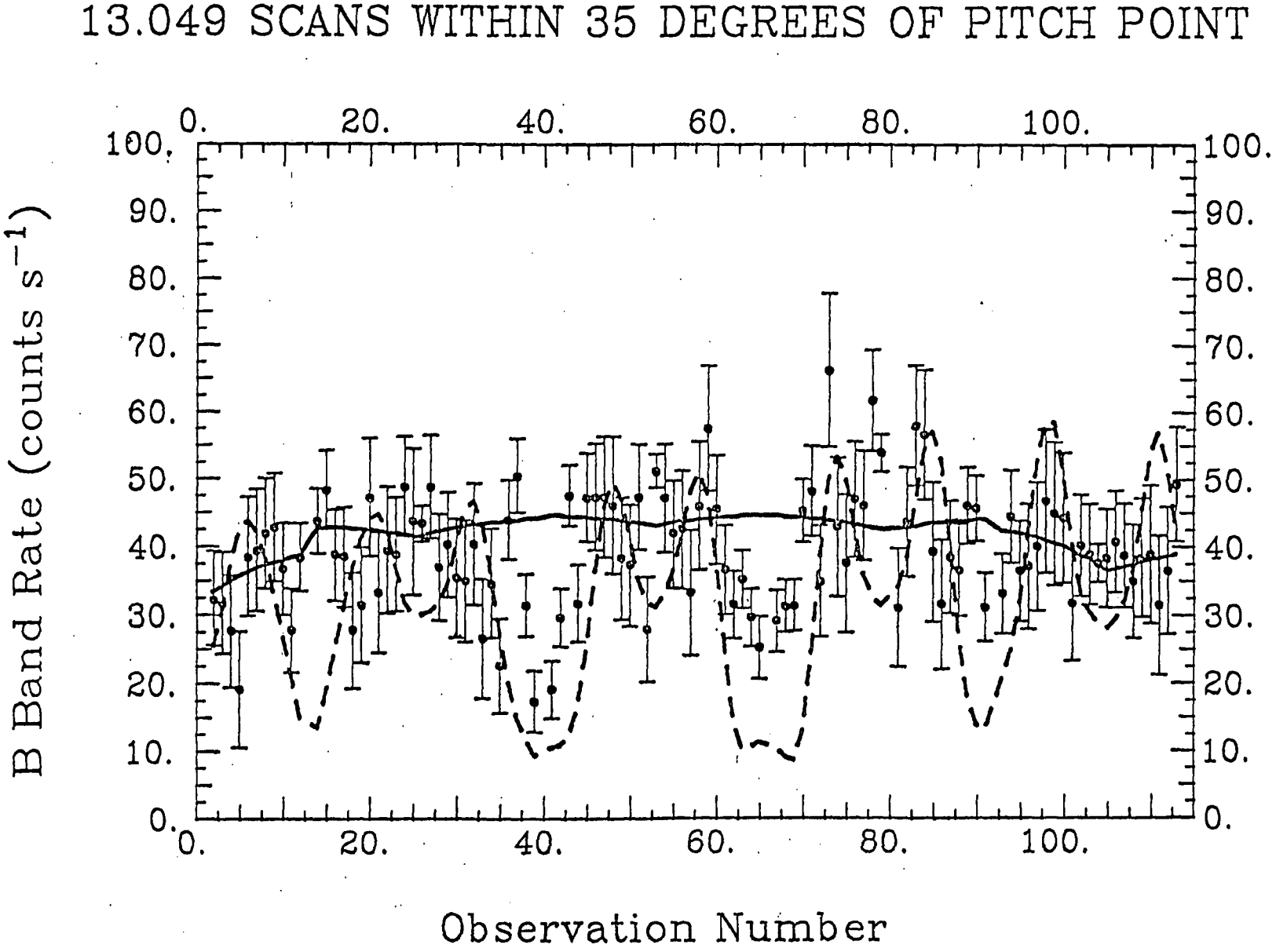
13.049 SCANS WITHIN 35 DEGREES OF PITCH POINT
B Band Rate (counts s^{-1})
Observation Number
0.
10.
20.
30.
40.
50.
60.
70.
80.
90.
100.

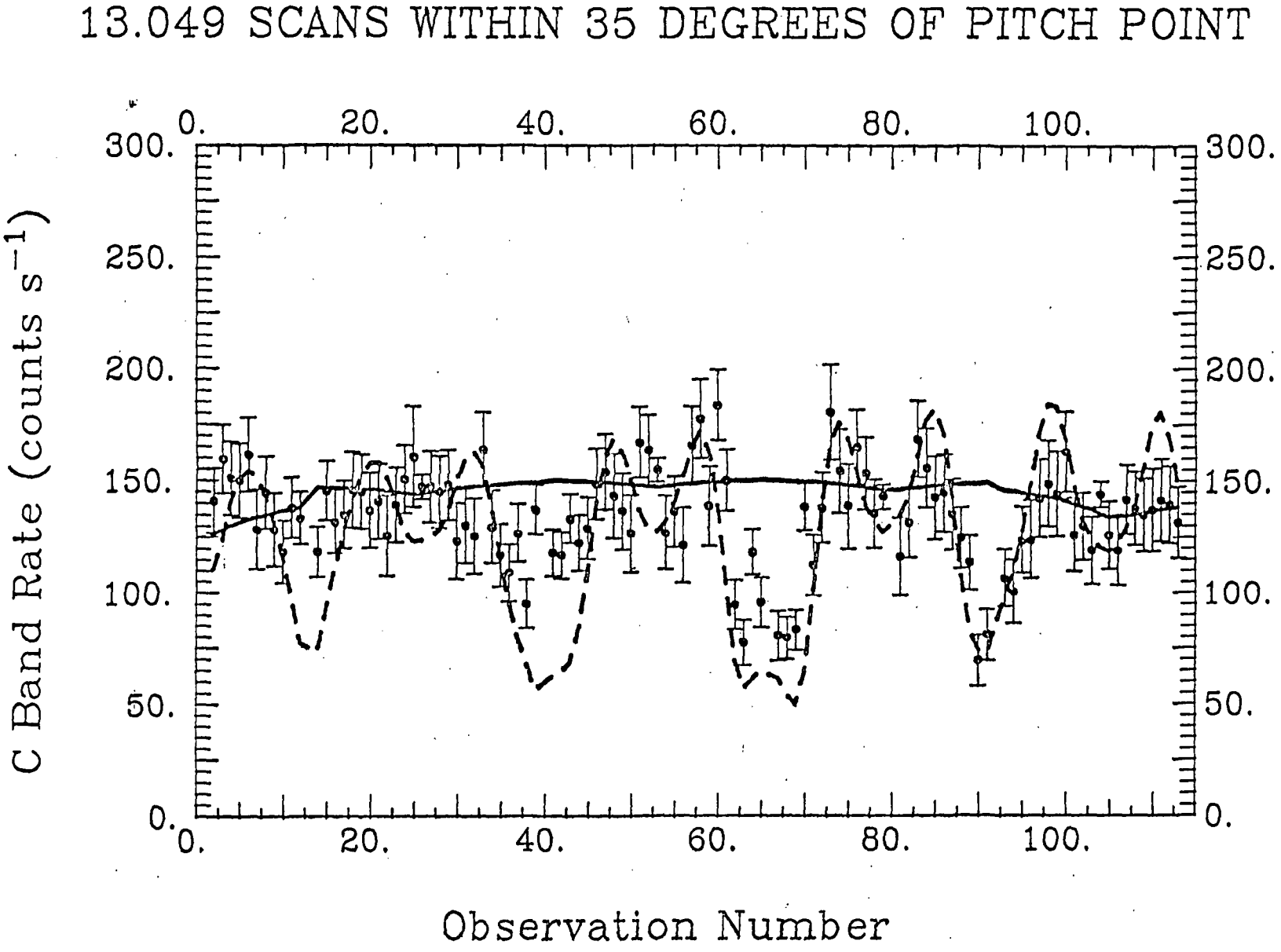
13.049 SCANS WITHIN 35 DEGREES OF PITCH POINT
C Band Rate (counts s^{-1})
Observation Number
0.
20.
40.
60.
80.
100.
300.
250.
200.
150.
100.
50.
0.